Journal of Computer Science

Research Article

Optimized Feature Selection for Kidney Ultrasound Image Classification Using Binary Coati Weighted Mean Vector Algorithm

Fizhan Kausar and Ramamurthy B.

Department of Computer Science, CHRIST (Deemed to be University), Bangalore, India

Article history
Received: 06-01-2025
Revised: 19-06-2025
Accepted: 04-08-2025

Corresponding Author:
Fizhan Kausar
Department of Computer Science,
CHRIST (Deemed to be University)
India
Email:
fizhan.kausar@res.christuniversity.in

Abstract: The analysis of medical images presents many challenges, especially when making precise diagnoses. In pediatric Chronic Kidney Disease (CKD), early identification is critical because of its gradual progression to significant kidney failure. This study proposes a diagnostic framework for pediatric ultrasound image classification that incorporated machine learning and advanced feature selection methods. This approach is divided into four stages: Preprocessing, feature extraction, feature selection, and classification. Initially, pediatric kidney ultrasound images are enhanced using gaussian median filter. Radiomics features were then extracted, including Gray Level Co-Occurrence Matrix (GLCM), Gray Level Size Zone Matrix (GLSZM), Gray Level Run Length Matrix (GLRLM), Neighboring Gray Tone Difference Matrix (NGTDM), Gray Level Dependence Matrix (GLDM), and first-order statistics. To optimize this feature space, we introduce the Binary Coati Weighted Mean Vector (BinCoWmv) optimization algorithm, which uses a customized fitness function. Herein, the selected features were evaluated using different classifiers: Random Forest (RF), Decision Tree (DT), Support Vector Machine (SVM), Naïve Bayes (NB), K-Nearest Neighbor (KNN), and XG-Boost. Comparative evaluations with existing optimizers, such as the Coati Optimization Algorithm (COA), weighted average vector (INFO), Firefly Algorithm (FFA), and Harris Hawk Optimization (HHO), showed that BinCoWmv achieved a higher classification accuracy. Our framework improves diagnostic reliability and assists radiologist and nephrologist in the early detection of chronic kidney disease in children.

Keywords: Kidney, Ultrasound, Feature Selection, Coati Optimization Algorithm, Weighted Mean Vector (INFO)

Introduction

The kidneys are essential organs that maintain the body's balance by filtering waste products from the blood, controlling blood pressure, regulating Ph levels, producing hormones, and maintain proper mineral concentration. Nowadays, the world is suffering from different kidney abnormalities that include children and adults (Dey *et al*., 2022). Chronic Kidney Disease (CKD) often starts with no specific symptoms and develops in uremic syndrome by the time the medical diagnosis has started (Badawy *et al*., 2023). But CKD in pediatrics starts due to a number of reasons that include congenital abnormalities, urinary tract problems, kidney infections, genetic disease, dehydration, and high blood pressure. Projections indicate that by 2040, CKD will be the fifth leading cause of death worldwide. However, research has shown that timely diagnosis and effective management can significantly slow its progression and prevent kidney failure (Francis *et al*., 2024). By employing Computer-Aided Diagnosis (CAD), the planned selection of materials can support nephrologists by offering accurate, reliable, and specific scans, thereby promoting earlier clinical decision-making.

SCIENCE Publications

With the development and application of Artificial Intelligence tools inherent in computer vision, which can analyze and solve medical image processing, have easier diagnosis. The use of these tools has been widely used in classification, detection, segmentation and object detection (Vasanthselvakumar *et al*., 2017). Then the diagnosis of kidney disease in pediatrics by ultrasonography is considered as a precise characterization of the disease, with gray scale ultrasound alone is difficult, even though the technique is non-invasive, while being considered as the safest medical imaging procedure and making it easier to distinguish between normal and abnormal kidney images (Bhandari *et al*., 2023).

Ultrasound image analysis often relies heavily on the expertise of sonologists and nephrologists, where minimizing human errors is essential for an accurate diagnosis. However, the quality of ultrasound images can sometimes be compromised by speckle noise, making it difficult for practitioners to identify specific diagnosis features of the images (Al-karawi *et al*., 2021). To overcome this problem, we extracted various texture features such as Gray level Co-Occurrence Matrix (GLCM), Gray Level Size Zone Matrix (GLSZM), Gray Level Run Length Matrix (GLRLM), Neighboring Gray Tone Difference Matrix (NGTDM), and Gray Level Difference Matrix (GLDM) features and first order derivatives from pediatric ultrasound images. This study aims to enable the early identification of kidney abnormalities in children, which is crucial for timely medical intervention and can significantly enhance long-term health outcomes and survival rates for those affected.

The potential of the classifier mainly depends on the feature extracted from ultrasound images. However, the is quite prominent that not all the extracted features contribute to the classification process. By eliminating the redundant and irrelevant features, optimization algorithm for feature selection have emerged as the most effective tool in medical imaging that could reduce high dimensionality and improving the classification process (Pradeepa and Jeyakumar, 2023).

Feature Selection (FS) is termed to be a challenging and expensive two-way step process; one is creating a subset feature and the second is evaluating it. Based on the evaluation, FS is classified into filter, wrapper, and embedded methods (Nadimi-Shahraki *et al*., 2022). Filter method such as correlation coefficient, information gain, chi square test picks features based on the relevance of feature, via univariate statistics, whereas the wrapper method selects the features based on their usefulness in the classification performance. Embedded method combines the principle of filter and wrapper approaches by incorporating feature selection directly into the model-training process, thereby enhancing the overall performance of the classifier (Dyoub and Letteri, 2023; Seyyedabbasi, 2023).

Feature Selection (FS) can be expressed as a combinatorial or binary optimization problem in which a feature is either chosen or discarded. The primary goal is to reduce the number of selected features while simultaneously improving or at least preserving the classification accuracy (Barrera-García *et al*., 2023). In bio-medicine, metaheuristics algorithms are termed to be as optimization tool that can solve the FS problem effectively, these algorithms use various techniques to increase the efficiency of the search process (Aljarah *et al*., 2018). Several metaheuristics algorithms are proposed over the year that can solve FS problem such genetic algorithm, Particle Swarm Optimization (Mirjalili and Lewis, 2013), Ant Colony optimization (Wen *et al*., 2008), Grey Wolf optimization (Raju *et al*., 2018), Harris Hawk Optimization (Peng *et al*., 2023), Whale Optimization (Eid, 2018), Cat Swarm Optimization (Seyyedabbasi, 2023), Dragonfly optimization (Mirjalili, 2016), Firefly optimization (Lambert and Perumal, 2022) to name a few, But yet they frequently suffer from premature convergence, unstable search trajectories and limited local refinement ability. This limitation is further amplified in binary search spaces relevant to FS tasks, maintaining a balance between two primary phases: Exploration and exploitation is crucial.

Despite the development of numerous metaheuristics algorithms, the exploration and exploitation phases are crucial for finding optimal solutions within the search space. When solving a search problem, it is essential to balance the exploration of new regions of the search space with a more focused investigation of promising areas. This strategy reduces the risk of becoming trapped in local optima, which are solution that may seem optimal within a limited region but fail to represent the true global optimum (Yildizdan and Bas, 2024).While exploration is to search intensively around the promising region, which can improve the quality of the solution. Balancing of the exploration and exploitation phase can enhance the effectiveness of the search algorithm (Hao *et al*., 2024; Hashim *et al*., 2023). According to the “No Free Lunch” theorem, no single optimization algorithm can perform optimally across all problem domains (Wolpert and Macready, 1997). To address this limitation, hybrid strategies are often employed, combining the strengths of different algorithms to improve their efficiency. Motivated by this principle, we propose a hybrid optimization method that integrates Binary Coati Optimization with the weighted mean of vectors (INFO) algorithm, designed to enhance both feature selection and classification performance.

Metaheuristic algorithm names Coati Optimization Algorithm (COA) was proposed by Dehghani *et al*. (2023) based on swarm intelligence-based algorithm, that mimics coatis' natural behavior. They use two strategies: A hunt and attack strategy on the iguana known as exploration, and a process of escape from predators, known as exploitation. COA appear to be competitive when compared to well know metaheuristic algorithms, Nevertheless, COA have several limitations, as any other metaheuristics algorithms. Such as an imbalance between exploration and exploitation, premature convergence, gets easily stuck in local optima. To overcome limitation mentioned, it is inferred that the binary version of COA has great potential in solving combinatorial optimization tasks, we utilize COA with a distinct transfer function, named V-shaped transfer function to tackle combinatorial problem efficiently (Yildizdan and Bas, 2024).

Nonetheless, we have another optimizer, namely the weighted mean vector (INFO), which is detailed in (Ahmadianfar *et al.*, 2022). This method contributes to the development of a powerful hybrid optimization algorithm. The algorithm relies on three basic principles: Vector position update, vector combination, and a local search mechanism. To update the vector positions, the algorithm uses convergence acceleration and a mean-based rule. Afterwards, the updated vectors are concatenated to create a feasible solution. Finally, local search is used to improve utilization and eliminate less accurate solutions.

In the following study, we propose a methodology, Binary Coati Weighted Mean of Vector optimization algorithm known as BinCoWmv optimization algorithm, for FS, synergistically combines the exploration strength of the Binary Coati Optimization Algorithm (BinCo) with the adaptive local exploitation capability of the Weighted Mean Vector Strategy (INFO), by integrating this mechanism, BinCoWmv effectively balance global and local search dynamics within the binary feature space, enabling the identification of compact, high- quality feature subset optimizes the performance classification of abnormalities. To assess the effectiveness of the proposed method, the optimally selected feature subsets were evaluated across multiple classifiers using standard performance metrics, including accuracy, precision, recall, F1-Score, Receiver Operating Characteristic (ROC), and specificity.

The key contributions of the this research are as follows:

1. The Gaussian Median filter is employed to eliminate noise from images, CLAHE for contrast enhancement, while the Sobel Operator is utilized for detecting edges
2. Radiomics texture features such as first-order derivates and second order derivatives (GLCM, GLRLM, GLDM, GLSZM, NGTDM), extracted from the pediatric kidney ultrasound images, totalling 94 features
3. A novel hybrid Metaheuristic algorithm called Binary Coati Weighted Mean Optimization Algorithm (BinCOWmv Optimization Algorithm) is proposed, combining the Binary Coati Optimization algorithm and the Weighted Mean of Vectors (INFO) method for effectively selecting texture features for classification of kidney ultrasound images into normal and abnormal
4. The best features are evaluated using Random Forest, and the results are compared with other classifiers namely, RF, DT, KNN, SVM, NB, and XG-Boost, based on accuracy, precision, recall, f1-score, ROC, and specificity parameters
5 A comprehensive comparison was conducted against standalone FS methods, including COA, INFO, Harris Hawk Optimization (HHO), and Firefly optimization Algorithm (FFA)

Literature Review

Exploring the combination of radiomics with ultrasound images has gained considerable traction in kidney ultrasound images. Numerous studies have explored handcrafted, statistical and radiomics extracted features in combination with machine learning or deep learning techniques to improve the diagnosis of chronic kidney disease, with varying degres of effectiveness.

Tian *et al*. (2024) aim to assess the effectiveness of ultrasound imaging in detection of CKD. While considering the gray-level aspect of US images in the diagnosis, feature extraction was performed using CNN, whereas the screening model was used along with texture features and the ResNet34 deep learning model that could identify CKD and its stages.

Addressing the gap in chronic kidney disease, where most of the focus is on the adult population, often ignores the physiological differences between adults and children. Kou *et al*. (2024) bridges the gap by developing a non-invasive diagnostic model for children glomerulonephritis classification using ultrasound images; for preprocessing and segmentation, the images were standardized to 512 × 512 pixels, manual pixel-level segmentation was performed using the LabelMe tool to extract the region of interest; to enhance the model generalization, data augmentation was performed using random resizing, cropping, flipping, and photometric distortion techniques; Image segmentation was performed with precision using the U-Net model, while radiomics features were extracted from the identified region of interest for feature extraction and selection purposes. Statistical method Analysis of Variance (ANOVA) was used, and LASSO was used for dimensionality reduction. From the selected features, the random forest algorithm was applied to generate the classification model.

To enhance early detection of CKD, Patil and Choudhary (2024) proposed a novel approach for predicting CKD using a hybrid classification framework, an improved Gaussian filter was applied to remove noise and improve image quality. Watershed-based algorithm used for segmentation, mean intensity, regions of interest, and the proposed local vector model features are extracted from the segmented images. The extracted features served as input to the hybrid classification model, which included an optimized neural network and a Long-Short-Term Memory (LSTM) network, and the cat swarm optimization algorithm was used to fine-tune the neural network weights.

Integrating advanced machine learning techniques for the diagnosis of CKD, researchers aim to address the gap of traditional methods suffering from low accuracy, ineffective data dimensionality handling. In the developed classification model, Deepika *et al*. (2023) focuses on improving the FS process. For handling unbalanced data and missing values, normalization was applied, outlier checking for noise reduction technique, to identify the most important features of the fruit fly optimization algorithm, and a heterogeneous modified artificial method combining a combination of support vector machine, multilayer perceptron, and backpropagation method was proposed.

A new method is presented by Biradar *et al*. (2022) for classifying kidney conditions (stones, cysts, and normal tissue) by proposing a hybrid approach of feature extraction and classification of digital kidney ultrasound images. The suggested method employs the contourlet transform for noise reduction in images. Following this, histogram equalization is applied to enhance image quality. The process then involves automatic segmentation to isolate the Region of Interest (ROI). Subsequently, various features are extracted, including Haralick, shape, wavelet, Tamura, and HOG. These extracted features are then individually input into classifiers for the purpose of classification.

Overcoming the research gap in the application of radiomics in CKD assessment using ultrasound images, Bandara *et al*. (2022) explored the capabilities of radiomics features derived from ultrasound images of the kidney. The study extracted 465 radiomics features, encompassing both first-order and second-order gray-level statistical measures. Following this, a random forest algorithm was employed to identify the most effective features from the extracted set. The Gini index was utilized to evaluate the significance of each feature, resulting in the selection of the top 10 features. These chosen features were then used to train a Support Vector Machine (SVM) for classification purposes.

In the study by Tsai *et al*. (2022), pediatric kidney ultrasound images were classified as normal or abnormal, while the abnormalities included different classes, such as stone cysts, hydronephrosis, space-occupying lesions, and hyperechogenicity. The proposed model underwent preprocessing to standardize the input image dimensions. The ResNet-50 architecture and CNN were pretrained on the ImageNet dataset, and transfer learning was subsequently used to redefine the final connecting layer for the binary classification of normal and abnormal images using ResNet-50.

Kim and Ye (2021) utilized ultrasound images to classify the severity of kidney abnormalities into three classes, normal, mild, and moderate and severe, while in the study ROI recognized the cortex, medulla, cortex, and medulla of the kidney, features were extracted from the same, using the GLCM algorithm; 57 features were extracted including the size of the kidney, which is crucial in diagnosis; 58 input nodes, 10 hidden layers, and 3 output layers were constructed using ANN for classification.

The objective of the research proposed by Priyanka and Kumar (2020) was to develop a classification model for kidney images by extracting texture features and selecting the best subset to enhance classification accuracy. The researchers used ultrasound images of kidneys to extract GLCM features, which offer crucial insights into texture patterns. To reduce the dimensionality and computational complexity of the feature set, PCA was employed. PCA identified the 12 most significant features out of the original 44, retaining most of the data's variance. This reduced feature set was then used to train an ANN for classification, achieving a classification accuracy of 77.8% with PCA and 53.3% without PCA.

Nithya *et al.* (2020) focused on the application of machine learning techniques in medical image processing. The research proposes a novel hybrid method combining ANN for classification and multi- kernel k-means clustering for segmentation, the research highlights the importance of GLCM for detecting kidney abnormalities. To enhance the performance, the Crow Search Optimization Algorithm (CSOA) is used for feature selection. The experimental results showed that the proposed method achieves a maximum accuracy of 93.45%.

A novel method for predicting kidney disease using ultrasound and an Artificial Neural Network (ANN) has been introduced by Balamurugan and Arumugam (2020). This approach involves four steps: Initially, images undergo pre-processing with an optimal wavelet and bilateral filter. Subsequently, GLCM features are extracted from each image, and the most significant features are selected through the oppositional grasshopper optimization algorithm. Finally, the ANN is employed to classify the images as either normal or abnormal. The proposed system achieves a peak accuracy of 95.83%. This research investigated the use of texture analysis for categorizing kidney disease across various stages. The methodology employed in the study by Ahmad and Mohanty (2021) encompassed several steps: Preprocessing, which included speckle noise elimination and contrast enhancement; segmentation to extract regions of interest; feature extraction utilizing GLCM to capture spatial relationships between pixel intensities and wavelet transform; and classification. The final step involved applying machine learning algorithms, specifically ANN and SVM, to classify the trained selected features. Alkordy *et al*. (2023) provided a technique for the classification of kidney ultrasound images based on the stages, addressing the research gap of identifying CKD early stages by integrating Deep CNN, specifically VGG16, and PCA for feature extraction, and the performance of the model was assessed using metrics such as accuracy, precision, recall and F1score. A comparative summary of recent studies in kidney ultrasound classification is presented in Table 1, outlining their feature extraction, selection, dataset types, classifier performance, and limitations this table highlights the limited use of texture features in classification, especially in pediatric contexts.

Existing research on kidney disease classification often integrates deep learning, radiomic, and other features, but tends to overlook the standalone diagnostic significance of texture features in pediatric ultrasound. On the other hand, meta-heuristic methods like Coati Optimization Algorithm (COA) and INFO (weighted average of vector optimization) have yielded encouraging outcomes for FS tasks. COA has been employed in breast cancer classification using transfer learning to enhance model precision (Emam *et al*., 2024). Enhanced versions of Coati, such as dynamic COA and elite opposition COA, have been utilized on benchmark and biomedical datasets, showing an improved balance between exploration and exploitation (Qtaish *et al*., 2025; Wang *et al*., 2022). Likewise, INFO has been used for FS on microarray genetic data and EEG signal classification (Osama *et al*., 2023; Wang *et al*., 2022) demonstrates its capability to manage high-dimensional inputs effectively. Nonetheless, no current research integrates COA and INFO into a unified binary hybrid optimization algorithm framework. Additionally, earlier studies have predominantly concentrated on structural tabular datasets for FS, with limited exploration of texture-rich FS-based medical images.

Table 1: Detailed description of literature review

Reference	FS techniques used	Data type and Size	Features extracted and count	Accuracy	Limitations
(Tian *et al*., 2024)	CNN (No FS)	Ultrasound, 1456 images	Deep features (Resnet-34)-GLCM, HOG	Not reported	NO FS strategy: Potential overfitting
(Kou *et al*., 2024)	LASSO	Pediatric glomerulonephritis, 469 images	Radiomics (ROI)-1422 features	95.16%	Statistical FS lack adaptability; manual segmentation
(Patil and Choudhary, 2024)	None	Ultrasound, 137 images	Local vector model+ ROI + mean intensity-based features	94.08%	FS not optimized, heuristic tuning
(Bandara *et al*., 2022)	Random Forest +Gini index	Ultrasound radiomics, 102 images	Radiomics (1st& 2nd order)-465 features	93.73%	No optimizer; high dimensionality retained
(Kim and Ye, 2021)	GLCM	US Kidney (3 class: Normal/Mild/Severe) -471 images	GLCM+ Size metrics-57 features	95.4%	Manual ROI; no optimization
(Priyanka and Kumar, 2020)	PCA	Ultrasound (Normal, Kidney stone, cysts tumor)	GLCM,44 features	77.8%	Optimization and other classifier need to be applied to check the robustness of the proposed approach
(Nithya *et al*., 2020)	Crow search optimization algorithm	Ultrasound (stone, tumor), 100 images	GLCM, 22 features	93.45%	Limited dataset may have led to overfitting
(Alkordy *et al*., 2023)	PCA	Ultrasound (normal, stone, hydrops and cysts), 1260 images	VGG-16 features	92.11%	Classifier not clearly defined
(Balamurugan and Arumugam, 2020)	Oppositional Grasshopper optimization algorithm	Ultrasound, 1000 images	GLCM, 22 features	95.83%	Research does not explicitly provide recall, f1 score or AUC

This research is dedicated solely to estimating texture features and feature extraction by introducing the binary hybrid metaheuristics feature selection algorithm, BinCoWmv, which merges Binary Coati Optimization with the Weighted Mean Vector method. The proposed approach effectively identifies highly correlated features, enhancing the classification process while preserving the simplicity of the model.

Methods

This section outlines methodological framework for classifying pediatric kidney ultrasound images using an optimized feature selection strategy. The proposed pipeline combines image processing, radiomics-based texture feature extraction, a novel hybrid feature selection algorithm (BinCoWmv), and a machine learning classifier to facilitate early detection of pediatric renal abnormalities. Figure 1 displays the workflow diagram of the proposed system for organizing pediatric kidney ultrasound images. The following subsections provide a step-by-step explanation of each component of the methodology.

Dataset Description

For the following research work, acquiring the dataset of pediatric kidney ultrasound images was a tedious task, as there are no standard datasets offered for this purpose. Therefore, it was necessary to gather images for the dataset from the ultrasound case site (Shankar, 2024). For our study, we collected images of various kidney cases from pediatric ultrasound examinations, considering the age group from 3 weeks to 7 years old. In total 340 images of both normal and abnormal cases.

This Process synthetically generated additional samples for the minority (Normal) class based on nearest neighbor interpolation, resulting in a balanced dataset of 477 images-238 normal and 239 abnormal. Subsequently, the data were partitioned using a stratified 70:30 split, where 70% for training, 30% for testing. Ensuring that the class distribution was maintained across the subset and improving the reliability of the performance evaluation across classifiers, a detailed description of the preprocessing is mentioned in the following research paper (Kausar and Ramamurthy, 2023).

Feature Extraction

In the proposed study, we have extracted 94 image characteristics, encompassing both primary and secondary texture measurements from the Pyrandiomics library (Van Griethuysen *et al*., 2017). Primary features evaluate the distribution of voxel intensities, whereas texture measurements assess the spatial arrangement of these intensities. The analysis incorporated a wide range of texture metrics, including features derived from Gray-Level Co-occurrence Matrix (GLCM), Gray-Level Size Zone Matrix (GLSZM), Gray-Level Run Length Matrix (GLRLM), neighboring gray-tone difference matrix (NGTDM), Gray-Level Difference Matrix (GLDM), and first-order derivatives. This comprehensive approach enhanced the thoroughness of feature extraction. A concise Table 2 outlines the textural characteristics and their properties utilized in this research.

Table 2: Outline of texture features extracted and its description

Feature group	Count of features	Description	Relevance
First-Order	19	Statistical measure of pixel intensity is calculated, such as mean, entropy percentile	To measure the overall strength properties, including the uniformity of tissue in the area
GLCM	24	It studies image texture based on the spatial relationship between pixels, includes features such as contrast, correlation, joint entropy.	Helpful for recognizing regions with different textures and designs
GLRLM	16	It calculates the occurrence of gray level values and their path for different combination, includes features such as short or long run emphasis	Determine the form or resemblance of the components, particularly if they are alike.
GLSZM	16	Counts the occurrence of gray level in the images, feature including zone size and zone percentage	Helpful for identifying regions where pixel values are concentrated, which might suggest tissue patterns.
GLDM	14	Quantifies the relationship between gray level within connected to centre pixel, considering features with low and high dependency emphasis	Illustrates the connection between pixel brightness levels and might indicate subtle differences in tissue.
NGTDM	05	Determines the variance between individual pixel grayscale values and the mean grayscale pixel value, encompassing characteristics such as intensity, intricacy, and activity level.	Highlight the area with high and low intensity variations

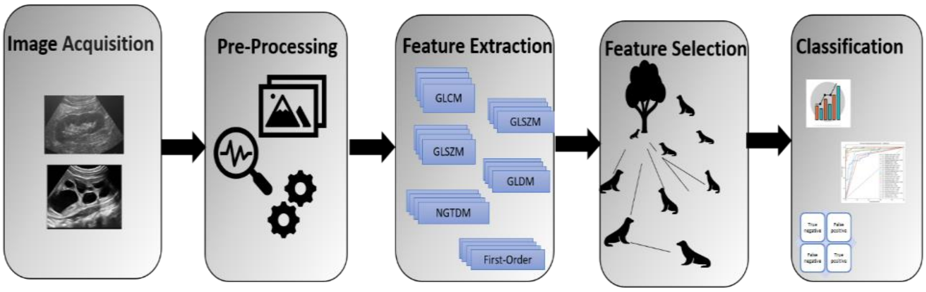

Fig. 1: Proposed methodology framework

Feature Selection

Coati Optimization Algorithm (COA)

The COA, introduced by Dehghani *et al*. (2023), is inspired by the natural foraging and social behaviors of coatis. In this algorithm, each coati represents a member of the population. A key advantage of the COA is that it operates without any algorithm-specific control parameters, which enhances its simplicity and makes it effective for tackling high dimensional and complex optimization problem.

The development of the metaheuristic algorithm is based on their predatory actions and strategies to avoid becoming prey. It simulated two specific behaviors: Predation, iguana attack, and avoidance of attack by their own predators. Behavior of the coatis are mathematically formulated sequentially below.

Initialization of Coati Swarm

The COA process begins by randomly initializing the position of the coatis within the search spaces. The position of the i^{th} in the j^{th} dimension is mathematically defined using the Eq. 1:

$$CO_{i_j} = LO_j + r.\left(UP_j - LO_j\right) \tag{1}$$

Where CO_{ij} represents the position of the i^{th} coati, r is a random real number in the range (0,1), and UP_j and LO_j : the upper and lower bounds of the j^{th} decision variable respectively.

Phase 1: Hunting and Attacking on Iguana (Exploration)

In this phase, the coatis mimic their natural hunting strategy by dividing into two groups. One group climbs tree to frighten the iguana, while other group waits below to capture the prey. This Cooperative behavior models the exploration process, enabling the algorithm to search diverse region of the solution space, as mathematically formulated in Eq. 2:

$$CO_j^{p_1} = CO_{ij} + Ra.\left(Iquana_j - I.CO_{ij}\right) \tag{2}$$

Where $CO_j^{p_1}$ denotes the new position of the i^{th} coati, CO_{ij} represents the current position of the i^{th} coati in the j^{th} dimension, I is a random value, Ra is another random variable, and $Iguana_j$ indicates the position of the iguana in the j^{th} dimension.

The second group models the random falls fo the iguana using Eq. 3:

$$Iguana^G = LB_j + Ra(UP_J - LO_J) \tag{3}$$

The position is adjusted according to the comparison of fitness between the current and new position using Eq. 4:

$$CO_i^{P1} = \begin{bmatrix} CO_{ij} + r.\left(Iguana - I.CO_{ij}\right), F_{iguana} < F_i \\ CO_{ij} + Ra.\left(CO_{ij} - Iguana_j\right), else \end{bmatrix} \tag{4}$$

Where $Iguana^G$ denotes the position of the iguana, F_{iguana} represents the objective function value of Iguana, and F_i is the objective function value of the i^{th} coati.

Phase 2: Escaping from predatory (Exploitation)

This phase illustrates the coatis' tendency to avoid danger by seeking refuge. They head towards a secure spot within their immediate vicinity. The size of this local area is adjusted dynamically according to the current iteration number t:

$$LO_j^{local} = \frac{LO_j}{t},\ UO_j^{local} = \frac{UO_J}{t} \tag{5}$$

The new position is computed as in Eq. 6:

$$CO_i^{P2} = CO_{ij} + (1 - 2Ra).\left(LO_j^{local} + Ra.\left(UP_j^{local} - LO_j^{local}\right)\right. \tag{6}$$

Where CO_i^{P2} defines the updated position of the coati, LO_j^{local} the local minimum bound of the j^{th} decision variable, UO_j^{local} denotes its local maximum bound, and t corresponds to the current iteration index.

Phase 3: Selection Mechanism

A greedy strategy is applied to preserve the most promising solutions, whereby a new position is accepted only if it improves the fitness value, as defined in Eq. 7:

$$CO_i^{P2} = \begin{bmatrix} CO_i^{P2}\ , F_{iguana}^{P2} < F_i \\ CO_{ij}\ else \end{bmatrix} \tag{7}$$

Where CO_i^{P2} is j^{th} dimension, F_{iguana}^{P2} represents objective value function.

After the coatis in the population have undergone position placement according to the algorithm's phases, from updating the population in equations 2 through 7 to identifying the remaining coatis in the search space and reaching the final iteration, the COA presents its output as the optimal solution across all iterations.

Weighted Mean Optimization Algorithm (INFO)

The Weighted Mean of Vectors (INFO) algorithm, proposed by Ahmadianfar *et al*. (2022) is a population-based optimization technique designed to tackle complex search problems using a dynamic vector-driven strategy. The algorithm proceeds through three main stages: A vector construction mechanism, a vector assembly phase, and a local search process. Its central principle lies in improving the population by computing a weighted mean of candidate's solutions, after which unfit vectors are replaced or refined. This process strengthens the global search capability while preserving local optimality.

Initialization Stage

The INFO algorithm, the population of vectors NP is distributed within a D0dimensional search space, expressed as:

$$(X_{l,j}^g = x_{l1}^g, x_{l2}^g, x_{l3}^g, \ldots., x_{lD}^g\}, l = 1,2,\ldots,N_P)$$

Theo key parameters govern the process: The weighted average factor (δ) and the scaling factor, which refine the updated vectors in line with the search domain. These parameters are computed adaptively, often through an exponential formulation, ensuring they remain consistent with the feasible search boundaries. Unlike algorithms that reply on user-defined settings, INFO adjusts these parameters dynamically. The algorithm begins by randomly initializing the vector population, thereby establishing diversity in the initial search.

Phase 1: Updating Rule

The INFO algorithm employs a distinctive update strategy that encourages diversity among the population while utilizing the weighted mean of vector to create new vectors. This algorithms unique method is founded on two core principles. The first principle involves a rule bases on the mean, derived from a weighted average of randomly chose vectors within the population. The second principle focuses on accelerating convergence, which aims to enhance the algorithms speed and efficiency, ultimately aiding in the identification of the optimal solution.

The Mean Rule (MR) is defined as follows:

$$MR = r \times M1_l^g + (1 - r) \times M2_l^g \text{ where l = 1,2,3…,N}_\text{p} \tag{8}$$

Where:

$$\mathrm{M1}_\mathrm{l}^\mathrm{g} = \delta \times \frac{w_1(x_{a1} - x_{a2}) + w_2(x_{a1} - x_{a3}) + w_3(x_{a2} - x_{a3})}{w_1 + w_2 + w_3 + \varepsilon} + \varepsilon \times \mathrm{rand} \tag{9}$$

Where:

$$w_1 = \cos\left(\left(f\,(x_{a1}) - f(x_{a2})\right) + \pi\right) \times \exp\left(-\frac{f(x_{a1}) - f(x_{a2})}{\omega}\right) \tag{10}$$

$$w_2 = \cos\left(\left(f\,(x_{a1}) - f(x_{a3})\right) + \pi\right) \times \exp\left(-\frac{f(x_{a1}) - f(x_{a3})}{\omega}\right) \tag{11}$$

$$w_3 = \cos\left(\left(f\,(x_{a2}) - f(x_{a3})\right) + \pi\right) \times \exp\left(-\frac{f(x_{a2}) - f(x_{a3})}{\omega}\right) \tag{12}$$

$$\omega = \max(f\,(x_{a1}), f\,(x_{a2}), f\,(x_{a3})) \tag{13}$$

Where:

$$M2_l^g = \delta \times \frac{w_1(x_{bs} - x_{bt}) + w_2(x_{bs} - x_{ws}) + w_3(x_{bt} - x_{ws})}{w_1 + w_2 + w_3 + \varepsilon} + \varepsilon \times rand \tag{14}$$

Where:

$$w_1 = \cos\left(\left(f\,(x_{bs}) - f(x_{bt})\right) + \pi\right) \times \exp\left(-\frac{f(x_{bs}) - f(x_{bt})}{\omega}\right) \tag{15}$$

$$w_2 = \cos\left(\left(f\,(x_{bs}) - f(x_{ws})\right) + \pi\right) \times \exp\left(-\frac{f(x_{bs}) - f(x_{ws})}{\omega}\right) \tag{16}$$

$$w_3 = \cos\left(\left(f\,(x_{bt}) - f(x_{ws})\right) + \pi\right) \times \exp\left(-\frac{f(x_{bt}) - f(x_{ws})}{\omega}\right) \tag{17}$$

$$\omega = f(x_{ws}) \tag{18}$$

$$\delta = 2\beta \times -\beta \tag{19}$$

$$\beta = 2exp(-4 \times \frac{g}{Maxg}) \tag{20}$$

In the above context, *f(x)* represents the objective function, while w_1, w_2, w_2 denoten from the interval [0, 0.5] and ω serve wavelet functions. The variable r is a random value draw s as an adjustment factor for the expansion parameter. The term ε refers to a very small constant. The indices $a1 \neq a2 \neq a3 \neq l$ are distinct integers randomly selected from the range [1, N]. The notations x_{bs}, x_{bt}, x_{ws} corresponds to the best, better, and worst individuals in the population during the g^{th} generation, respectively, while Max $_g$ denotes the maximum number of generations.

Within INFO, CA facilitates the movement of vectors in various directions, striving to achieve an optimal solution. This process can be described as follows:

$$CA = randn \times \frac{(x_{bs} - x_{a1})}{(f\,(x_{bs}) - f\,(x_{a1}) + \epsilon)} \tag{21}$$

Hence, the new vector is defined as follows:

$$z_l^g = x_l^g + \sigma \times MR + CA \tag{22}$$

During the iterative process, a comprehensive global search is required to identify the most promising regions within the search space, a stage referred to as the exploration phase. In the INFO algorithm, these regions are represented by the vectors $\mathrm{x_{bs}}, \mathrm{x_{bt}}, \mathrm{x_{ws}}$, which corresponds to candidate solutions proposed in the *i*th iteration and are defined through specific mathematical formulations:

$$\left\{\begin{array}{c} \text{if rand} < 0.5 \\ \mathrm{z1_l^g = x_l^g + \sigma \times MR + randn}\ \frac{\mathrm{x_{bs} - x_l^g}}{(\mathrm{f\,(x_{bs}) - f\,(x_l^g)} + 1)} \\ \mathrm{z2_l^g = x_{bs} + \sigma \times MR + randn}\ \frac{\mathrm{x_{a1}^g - x_{a2}^g}}{(\mathrm{f\,(x_{a1}^g) - f\,(x_{a2}^g)} + 1)} \\ \text{else} \\ \mathrm{z1_l^g = x_a^g + \sigma \times MR + randn}\ \frac{\mathrm{x_{a2}^g - x_{a3}^g}}{(\mathrm{f\,(x_{a2}^g) - f\,(x_{a3}^g)} + 1)} \\ \mathrm{z2_l^g = x_{bt} + \sigma \times MR + randn}\ \frac{\mathrm{x_{a1}^g - x_{a2}^g}}{(\mathrm{f\,(x_{a1}^g) - f\,(x_{a2}^g)} + 1)} \end{array}\right. \tag{23}$$

In the *g*th generation, the newly generated vectors are denoted as $z1_l^g, z2_l^g$. The scaling rate of a vector, represented by σ, is calculated using Eq. 24:

$$\sigma = 2\alpha \times rand - \alpha \tag{24}$$

Where, α has the ability to modify its location using an exponential function, which is expressed as:

$$\alpha = c\ exp(-d \times \frac{g}{Maxg}) \tag{25}$$

Where α = 2 and d = 4 are constant numbers, it is worth noting that, if value of σ very large, the algorithm employs a larger step size, allowing the current vector to conduct a broad search. This results in the algorithm favouring exploration or else causing the current vector to perform a localized search. In this case, the algorithm leans towards the development phase.

Phase 2: Vector Combining Phase

In the second phase, vector merging is essential for boosting population diversity and enhancing the ability to conduct local searches. The newly created vectors $\mathrm{z1_l^g}$ and $\mathrm{z2_l^g}$ are merged to form new ones, which can potentially lead to improved solutions during the search process. This merging is illustrated by the equation given below:

$$\left\{\begin{array}{c} if\ rand < 0.5 \\ if\ rand < 0.5 \\ u_l^g = z1_l^g + \mu.\left|z1_l^g - z2_l^g\right| \\ else \\ u_l^g = z2_l^g + \mu.\left|z1_l^g - z2_l^g\right| \\ end \\ else \\ u_l^g = x_l^g \\ end \end{array}\right. \tag{26}$$

Where u_l^g denoted the newly generated vector in the *g*th.

Generation, and $\mu = 0.05 \times \mathrm{randn}$, with randn representing a normally distributed random value.

Phase 3: Local Search Strategy

The INFO algorithm employs a local search strategy to prevent stagnation in local optima and to strengthen exploitation, thereby improving convergence toward the global solution. This is achieved through a heuristic that generates a new vector. When r < 0.5, a candidate vector, denoted as x_{best}^g, is created around the current operator. In this context, rand represents a random value within the interval [0,1]. This stage of the process is defined as follows:

$$\left\{\begin{array}{c} \text{if rand} < 0.5 \\ \text{if rand} < 0.5 \\ \mathrm{u_l^g = x_{bs} + randn \times (MR + randn \times x_{bs}^g - x_{a1}^g))} \\ \text{else} \\ \mathrm{u_l^g = x_{bs} + randn \times \left(MR + randn \times (v_1 \times x_{bs} - v_2 \times x_{rnd})\right)} \\ \text{end} \\ \text{end} \end{array}\right. \tag{27}$$

Where:

$$\mathrm{x_{rnd}} = \emptyset \times \mathrm{x_{avg}} + (1 - \emptyset) \times (\emptyset \times \mathrm{x_{bt}} + (1 - \emptyset) \times \mathrm{x_{bs}} \tag{28}$$

$$\mathrm{x_{avg}} = \frac{(\mathrm{x_a + x_b + x_3})}{3} \tag{29}$$

$$\mathrm{v_1} = \begin{cases} 2 \times \text{rand if p} > 0.5 \\ \quad 1 \text{ otherwise} \end{cases} \tag{30}$$

$$\mathrm{v_2} = \begin{cases} \text{rand if p} < 0.5 \\ \quad 1 \text{ otherwise} \end{cases} \tag{31}$$

where, ∅ denotes a value randomly selected from the range of 0 to 1; v_1 and v_2 are two such random numbers as previously described and detailed description of the following optimization algorithm is described in following research work (Ahmadianfar *et al*., 2022).

Proposed BinCoWmv Optimization Algorithm (Binary Coati Weighted Mean Vector)

The BinCoWmv Optimization Algorithm process begins with the initialization of the coati population; in first phase the coati location is initialized:

$$C_{ij} = Lo_j + r.\left(Up_j - Lo_j\right) \tag{32}$$

Where C_{ij} denotes the position of the coati, r is a random value, and $Lo_j \ and \ Up_j$ represents the lower and upper bound of the jth decision variable, respectively. In this phase, the coatis split into two groups: One climbs the tree to chase iguanas, while the other waits on the ground to capture it. Based on this cooperative behavior, the iguana's position is updated according to the following Equations:

$$C_j^{new} = C_{ij} + Rv.\left(Iq_j - I.C_{ij}\right) \tag{33}$$

Where C_j^{new} is the new position of the ith coati, C_{ij} is the position of the ith coati in jth dimension, I is the random value, Rv is the random value, Iq_j is the location of the Iguana. The position of the coati is updated based on their random position:

$$Ig^G = Lb_j + Ra(Up_j - Lo_j) \tag{34}$$

$$\begin{bmatrix} C_{ij} + r.\left(Ig - I.C_{ij}\right), F_{Ig} < F\left(C_{ij}\right) \\ C_{ij} + Ra.\left(C_{ij} - Ig_j\right), else \end{bmatrix} \tag{35}$$

Where Ig^G is the location of the iguana, F_{iguana} is the iguana objective function, $F_i$is the objective function of the ith coati, the position of the iguana shows the best location.

In the second phase, the process involves updating rules and combining vectors. Rather than moving towards an improved solution, a set of randomly chosen coati differential vectors is used to calculate a weighted average. This phase considers population diversity through the Mean Rule, which is influenced by the better, best, and worst solutions. The better solution is identified by evaluating the objective value of the top-performing solution, and the $Mean_{Rule}$ is conducted based on the Eq. 36 defined:

$$Mean_{Rule} = \mathrm{rv} \cdot CWM_1 + \ (1 - \mathrm{r}) \cdot \ CWM_1 \tag{36}$$

$$CWM_1 = \ \delta \times \frac{w_1 \cdot (c_a - c_b) + w_2 \cdot (c_a - c_c) + w_3 \cdot (c_b - c_c)}{w_1 + w_2 + w_3 + \varepsilon} + \varepsilon \times r \tag{37}$$

Where:

$$w_1 = \cos((f_a - f_b) + \pi) \times \exp\left(\frac{f_a - f_b}{\omega}\right) \tag{38}$$

$$w_2 = \cos((f_a - f_c) + \pi) \times \exp\left(\frac{f_a - f_c}{\omega}\right) \tag{39}$$

$$w_3 = \cos((f_b - f_c) + \pi) \times \exp\left(\frac{f_b - f_c}{\omega}\right) \tag{40}$$

Where:

$$\omega_1 = \max(f_a, f_b, f_c) \tag{41}$$

$$f_a = f(C_a), f_b = f(C_b), f_c = f(C_c) \tag{42}$$

$$CWM_2 = \ \delta \times \frac{w_4 \cdot (C_{bs} - C_{bt}) + w_5 \cdot (C_{bs} - C_{ws}) + w_3 \cdot (C_{bt} - C_{ws})}{w_4 + w_5 + w_6 + \varepsilon} + \varepsilon \times r \tag{43}$$

Where:

$$w_1 = \cos((f_1 - f_2) + \pi) \times \exp\left(\frac{f_1 - f_2}{\omega_2}\right) \tag{44}$$

$$w_2 = \cos((f_1 - f_3) + \pi) \times \exp\left(\frac{f_1 - f_3}{\omega_2}\right) \tag{45}$$

$$w_3 = \cos((f_2 - f_3) + \pi) \times \exp\left(\frac{f_2 - f_3}{\omega_2}\right) \tag{46}$$

Where:

$$\omega_2 = \max(f_1, f_2, f_3) \tag{47}$$

$$f_1 = f(C_{bs}), f_2 = f(C_{bt}), f_3 = f(C_{ws}) \tag{48}$$

Where f_x is the objective function value, where a $a \neq b \neq c$ are the coatis randomly selected from the population, ε is very small constant value, r is the random value normally distributed, C_{bs} , C_{bs} , C_{bs} are the coati's best, better and worst solution among all the vectors in the population. Based on the iteration the solution is being determined, rv is the random value, w_1, w_2, w_3 are the WF's to calculate the weighted mean vector of the coatis, that help to search in the solution space globally. To discover promising search space, the updating is based on following condition:

$$\begin{cases} CO_{z1} = C_i + \ \sigma \ \cdot (rv \ \cdot Mean_{Rule}) + \frac{rv.(C_{bs} - C_a)}{f_1 - f_a + 1} \\ CO_{z2} = C_{bs} + \ \sigma \ \cdot (rv \ \cdot Mean_{Rule}) + \frac{rv.(C_a - C_b)}{f_a - f_b + 1} \\ \qquad else \\ CO_{z1} = C_a + \ \sigma \ \cdot (rv \ \cdot Mean_{Rule}) + \frac{rv.(C_b - C_c)}{f_b - f_c + 1} \\ CO_{z2} = C_{bt} + \ \sigma \ \cdot (rv \ \cdot Mean_{Rule}) + \frac{rv.(C_a - C_b)}{f_a - f_b + 1} \end{cases} \tag{49}$$

Where CO_1 and CO_2 represents the newly generated population vectors, σ is the scaling factor as defined in Eq 49 and α is an adaptive parameter that can be adjusted according to the exponential function specified in Eq. 50:

$$\alpha = c \ \exp(-d \times \frac{g}{Max_C}) \tag{50}$$

In the exploration phase of the BinCoWmv optimization algorithm, population diversity is enhanced by combining two coati vectors with the vector C_{ij}. When the condition rand <0.5 is satisfied, a new vector CV_{ij} is generated according to Eq. 51. This operator strengthens the local search capability, allowing the algorithm to introduce novel potentially more promising candidate solutions:

$$\begin{cases} if\ rand < 0.5 \\ if\ rand < 0.5 \\ CV_{ij} = CO_{z1} + \mu * |CO_{z1} - CO_{z2}| \\ else \\ CV_{ij} = CO_{z2} + \mu * |CO_{z1} - CO_{z2}| \\ end \\ else \\ C_{ij} = CV_{ij} \end{cases} \tag{51}$$

$$C_i = \begin{cases} CV_{ij}^{new}, F_i^{new} < F(C_{ij}) \\ C_{ij}\ else \end{cases} \tag{52}$$

Where CV_{ij} represents the vector generated through the combination process within the population, $\mu\ is\ set\ to\ 0.05$.

Lastly, in the third phase, the algorithm refines solutions by updating the positions of the coatis in the search space, simulating their response to an attack or threat form a predator:

$$local_{lb} = \frac{lb_j}{t}, local_{ub} = \frac{ub_j}{t} \tag{53}$$

$$C_i^{new} = C_{ij} + (1 - 2r) \cdot (local_j^{lb} + r \cdot \begin{pmatrix} local_j^{ub} - \\ local_j^{lb} \end{pmatrix} \tag{54}$$

Where C_i^{new} denotes the updated position of the ith coati in the third phase of *COA*, and C_i^{new} represents its position in the *j*th dimension. Here r is a random value, *t* indicates the current iteration, $local_j^{ub}$ and $local_j^{lb}$ define the local upper and lower bounds of the jth decision variable, while ub_j and lb_j, corresponds to the global upper and lower bounds of the *j*th decision variable, respectively.

Furthermore, to prevent coatis from becoming trapped in local optima, the mean rule defined in Eq. 36 is incorporated within the local search during the exploitation phase. This mechanism enhances both the search process and convergence towards the global optimum. Based on this operator, a new vector is generated using Eq. 55:

$$\begin{cases} if\ rand < 0.5 \\ if\ rand < 0.5 \\ CV_{ij} = C_{bs} + rand * (Mean_{Rule} + rand * (C_{bs} - f_a) \\ else \\ CV_{ij} = C_{bs} + rand * (Mean_{Rule} + rand * (v_1 * C_{bs} - v_2 * C_{rand}) \\ end \\ end \end{cases} \tag{55}$$

Where ∅ stands for random number between (0,1), C_{rand} is the new solution that combines the elements of the solution x_{avg}, C_{bs}, C_{bt}:

$$C_{rnd} = \emptyset \times C_{avg} + (1 - \emptyset) \times (\emptyset \times C_{bt} + (1 - \emptyset) \times C_{bs} \tag{56}$$

$$x_{avg} = \frac{(C_a + C_b + C_C)}{3} \tag{57}$$

The newly calculated and updated position to improve the objective function, simulated using the following condition:

$$C_i = \begin{cases} C_{ij}^{new}, F_i^{new} < F(C_{ij}) \\ C_i\ else \end{cases} \tag{60}$$

Here C_i^{new} represents the updated position of the coati as determined in the third phase of the BinCoWmv optimization algorithm, C_{ij}^{new} denotes its position in the jth dimension, F_i^{new} corresponds to its objective function value.

In medical feature selection problems, binary values 0 and 1 are used to represent whether a feature is excluded or selected. Since the proposed BinCoWmv optimization algorithm functions in a continuous search space, a transformation into binary search space is required. To achieve this, a V-shaped transfer function is applied during the exploration phase, with its formulation defined in Eq. 61:

$$\mathrm{T(x)} = |\tan(x)| \tag{61}$$

$$x_{Binary} = \begin{cases} 1\ if\ rv < X(x) \\ 0\ if\ rv \geq X(x) \end{cases} \tag{62}$$

Where $X(x)$ is the binary representation of the solution *P* produced by 61 and 62, rv ϵ [0,1] is random number. The Algorithm 1 describes the pseudocode of the BinCoWmv optimization algorithm.

Algorithm 1: Pseudocode of the proposed BinCoWmv Optimization Algorithm

```
**Start BinCoWmv Optimization Algorithm**
Input the information about the optimization problem
Set the no. of iteration T and population of the coati N
Initialize the position of the coati using Eq. 32 and evaluate the Objective function
For t = 1: T
Updating location of the iguana
**Phase 1: Exploration**
For i=1: [N/2]
Calculate the new position of i^th coati using Eq. 33
position of i^th coati is updated using Eq. 52
End for
For i=1+ [N/2]: N
Random position of iguana is calculated using Eq. 34
The new position for i^th coati is calculated using Eq. 35
**Phase 2: INFO rule**
Select coati randomly $a \neq b \neq c$ within range [1, N]
*Update rule stage*
 Calculate Vector of the coati $CO_{z1}$ and $CO_{z2}$ using Eq. 49
*Vector combing stage*
Calculate combing of coati's vectors using Eq. 51
Position of i^th coati is updated using Eq. 52
End for
```

```
Phase 3: Exploitation using local search operator
Calculate the bounds for the coatis using Eq. 53
For i=1: N
    New position of the coati's is calculated using Eq. 54
    Local search operator is calculated using the Eq. 55
    Update the $i^{th}$ coati position using the Eq. 60
End for
Best solution so far is saved
End for
Display the optimal coati result generated by BinCoWmv optimization algorithm.
```

Classification

Several widely-used classification algorithms for kidney ultrasound image analysis include RF, DT, SVM, NB, KNN, and XG-Boost, all of which were employed in our research. The RF classifier functions by aggregating the outputs of multiple decision trees to improve classification performance. It is versatile, working well with both small and large datasets. In contrast, DT is a simpler and faster model that can capture complex non-linear relationships, and it can effectively process both numerical and categorical data. SVM is an algorithm that performs well on unseen data, effectively managing both linearly and non-linearly separable data by employing kernel functions (RBF, sigmoid, poly, and linear) for nonlinear datasets. KNN is a simple, easily interpretable classifier that categorizes based on the k-value. NB, founded on Bayes' theorem, is uncomplicated and quick to train, functioning optimally with small datasets. XG-boost, a boosting classifier, offers flexibility in its objective function.

Results

The experiments were conducted on a high-performance workstation equipped with an Intel Core i9-13900K CPU, 64 GB DDR5 RAM, and an NVIDIA RTX A6000 GPU, ensuring fast and parallel processing of computationally intensive tasks. The system utilized a 1 TB NVMe SSD for high-speed operations and a 5 TB HDD for data storage, running on Windows 10 (64-bit). Python 3.10 was used for data preprocessing, feature extraction (via PyRadiomics), classification, and performance evaluation, while MATLAB R2023b facilitated the implementation and execution of metaheuristic optimization algorithms, leveraging its optimization and parallel computing toolboxes.

The application of the BinCoWmv optimization algorithm as a Feature Selection (FS) technique for categorizing pediatric ultrasound images. The dataset, obtained from an online source, consists of normal and abnormal kidney images from children aged 3 weeks to 7 years. A total of 94 texture features were extracted from the kidney ultrasound images, though not all features were crucial for classifying pediatric kidney images. The proposed method was employed for FS to enhance classification accuracy. The primary goal of this research was to minimize features while improving classification accuracy. Classifiers such as RF, DT, SVM, NB, KNN, and XG-Boost were employed with 5-fold cross-validation to evaluate with and without proposed FS method, and the parameters of the classifiers are mentioned in Table 3. Additionally, original optimization algorithms were applied using both the original features and those selected by COA, INFO, FFA, and HHO. To assess the effectiveness of the proposed BinCoWmv optimization algorithm, the experiment was conducted over pop size of 10, a dimension 30, 5 iterations, 30 runs, and 100 epochs; its parameters are mentioned in Table 4. Metrics used to evaluate classifiers include fitness measures, the performance of the classifier, and computational efficiency, which provide information about the behavior of the model. The description of the measure are as follows: Coati true positive (CT_p),coati true negative (CT_n),coati false positive (CF_p),coati false negative (CF_n).

Accuracy: To measure the accurate efficiency of the proposed system using the formula:

$$Accuracy = \frac{CT_p + CT_n}{CT_p + CT_n + CF_p + CF_n} \tag{62}$$

Precision: To measure no of positive class are accurate in the classification of images:

$$Precision = \frac{CT_p}{CT_p + CF_p} \tag{63}$$

Table 3: Parameters setting for classifiers used in the study

Classifiers	Hyperparameters
Random Forest (RF)	n_estimator=100, criterion=" gini"
Decision Tree (DT)	criterion=" gini", max_depth = 8, min_samples = 4
Naïve Bayes (NB)	GaussianNB
K-Nearest Neighbor (KNN)	K = 5, Weights ='distance'
Support Vector Machine (SVM)	Kernel = 'rbf, decision function= 'ovo', gamma = 100
Extreme Gradient Boost (XG-Boost)	Max_dept = 2, learning rate = 0.01

Table 4: Parameter setting of the algorithm used in the study

Algorithms	Parameter	Values
BinCoWmv (Proposed)	c, d	2,4
INFO	c, d	2,4
HHO	β_0 , α, γ	0.2, 1.0, 0.5
BCOA	Parameter free	-
FFA	Parameter free	-

Specificity: To measure the negative class in the classification of images:

$$\text{Specificity} = \frac{\text{CT}_\text{n}}{\text{CT}_\text{n}+\text{CF}_\text{p}} \tag{64}$$

Recall: To measure the positive rate in the classification of images:

$$\text{Recall} = \frac{\text{CT}_\text{p}}{\text{CT}_\text{p}+\text{CF}_\text{n}} \tag{65}$$

F-measure: To measure the test accuracy, to verify how well the test performs:

$$\text{Fmeasure} = 2 \times \frac{\text{Recall} \times \text{Precision}}{\text{Recall}+\text{Precision}} \tag{66}$$

Average Solution Time: The average time taken by the BinCoWmv for the computation in seconds, *T* times is determined as follows:

$$Average\ solution\ time = \frac{1}{T}\sum_{t=1}^{T} AvgSolnTime_c \tag{67}$$

Where $AvgSolnTime_c$ is the computational time at *t* run or iteration.

Best Fit: BinCoWmv derives the minimum fitness value, which computes as follows:

$$Best_{fit} = \min_{i\epsilon\{1,2,\ldots,N\}} \sum_{j=1}^{C_i} f(C_{ij}) \tag{68}$$

Worst Fit: BinCoWmv derives the maximum fitness value, which computes as follows:

$$Worst_{fit} = \max_{i\epsilon\{1,2,\ldots,N\}} \sum_{j=1}^{C_i} f(C_{ij}) \tag{69}$$

N denotes the total number of candidate solutions in the population. The index $i \in \{1, 2, \ldots, N\}$ represents the i^{th} candidate solution. C_{ij} refers to the j^{th} feature selected by the i^{th} candidate solution, while C_{ij} indicates the total number of features selected in the i^{th} solution. The objective function $f(C_{ij})$ evaluates the quality of the selected feature C_{ij}.

Average feature count: count on average BinCoWmv selects features is calculated as:

$$Avgerage\ selected\ feature\ = \frac{1}{T}\sum_{c=1}^{T} \frac{AvgCount^c}{N} \tag{70}$$

Where $AvgCount^c$ is the selected feature count, and *N* represents total number of features.

Mathews Correlation Coefficient (MCC): to evaluate the Corelation between the predicted and actual binary outcomes:

$$MCC_C = \frac{\text{CT}_\text{p} \cdot \text{CT}_\text{n} - \text{CF}_\text{p} + \text{CF}_\text{n}}{\sqrt{(\text{CT}_\text{p}+\text{CF}_\text{p})(\text{CT}_\text{p}+\text{CF}_\text{n})(\text{CT}_\text{n}+\text{CF}_\text{p})(\text{CT}_\text{n}+\text{CF}_\text{n})}} \tag{71}$$

Fitness Function: The fitness function assesses the trade-off between the classification error and the quantity of features chosen:

$$f = \alpha \cdot (1 - Accuarcy) + \beta \cdot \frac{|SF|}{|N|} \tag{72}$$

Where α and β are the weights of selection ratio, selected features quality. That fall within the range of [0,1], *SF* and *N* are the selected features and total features respectively and (1-accuracy) is the classification error obtained by the classifiers. The p-value obtained from Friedmans test is used to evaluate the validity of a hypothesis. A p-value below 0.05 is generally interpreted as significant evidence to reject the null hypothesis, indicating that the observed differences are unlikely to have occurred by chance.

The performances of the proposed Binary Coati Weighted Mean of Vector (BinCoWmv) optimization algorithm for feature selection were evaluated using metrics such as mean fitness, standard deviation of fitness, worst fitness values and number, selected features, computational time, and Matthew's Correlation Coefficient (MCC) as described in Table 5. As shown in Figure 5, the Random Forest (RF) classifier presented the lowest average fitness before feature selection, indicating an efficient cost function and robust base learning. The Naïve Bayes (NB) classifier displayed the highest average fitness, reflecting suboptimal initial performances. XG-Boost achieved a competitive fitness average of 0.01073. After applying the BinCoWmv feature selection, improvements were observed for all classifiers. RF and XG-Boost achieved an optimal fitness value of 0.01042. RF presented zero fitness variance, confirming its stability, with an increase in the number of selected features to 27.07. MCC values improved for all classifiers, RF reaching 0.9590, indicating reliable classification in the presence of class imbalance. Table 6 shows that RF outperforms the other classifiers, improving the accuracy from 94.41 to 96.50%, as confirmed by the confusion matrix in Figure 3. XG-Boost achieves an accuracy of 95.10% after feature selection, which is a decision that presents a better generalization. Naïve Bayes improves recall, but its precision remains lower, while SVM displays a slight improvement in recall. Figure 2 illustrates the improvement of ROC-AUC scores after feature selection for all classifiers. Despite the increased computational time, the gains in accuracy, Matthew's Correlation Coefficient (MCC), and model reliability justify this trade-off, especially for clinical decision support systems. Figures 4 and 5 demonstrate the comparative gains achieved by feature selection.

Table 5: Evaluation of classifiers of with / without FS across different classifiers for values: Mean, STD, Best fit, Worst fit, Avg Feature count, Avg Solution time, MCC, Fitness

	Classifier	Mean	Std	Best fit	Worst fit	Avg feature count	Avg solution time	MCC	Fitness
Without FS	DT	0.01976	0.00642	0.01001	0.02873	10.50000	0.01599	0.70700	0.01976
	RF	0.00902	0.00240	0.00575	0.01283	6.80000	0.18443	0.86010	0.00902
	SVM	0.06949	0.01072	0.05869	0.08458	14.10000	0.09920	0.27200	0.06949
	KNN	0.06674	0.01021	0.04884	0.08240	13.50000	0.00378	0.39900	0.06674
	NB	0.08475	0.01308	0.06669	0.10819	12.20000	0.00416	0.23220	0.08475
	XG-Boost	0.01073	0.00375	0.00564	0.01752	7.90000	0.33520	0.84610	0.01073
With FS (BinCoWmv)	DT	0.01563	0.00521	0.01042	0.02083	10.81078	178.20962	0.91746	0.02083
	RF	0.01042	0.00000	0.01042	0.01042	27.07243	325.22336	0.95903	0.01042
	SVM	0.04167	0.04501	0.00000	0.13542	29.14797	101.94759	0.93754	0.03125
	KNN	0.05469	0.05381	0.01042	0.14583	16.56446	98.00257	0.91946	0.04167
	NB	0.05903	0.06153	0.01042	0.14583	19.88417	119.84259	0.70794	0.14583
	XG-Boost	0.04375	0.04904	0.01042	0.13542	29.38760	119.40345	0.94648	0.01042

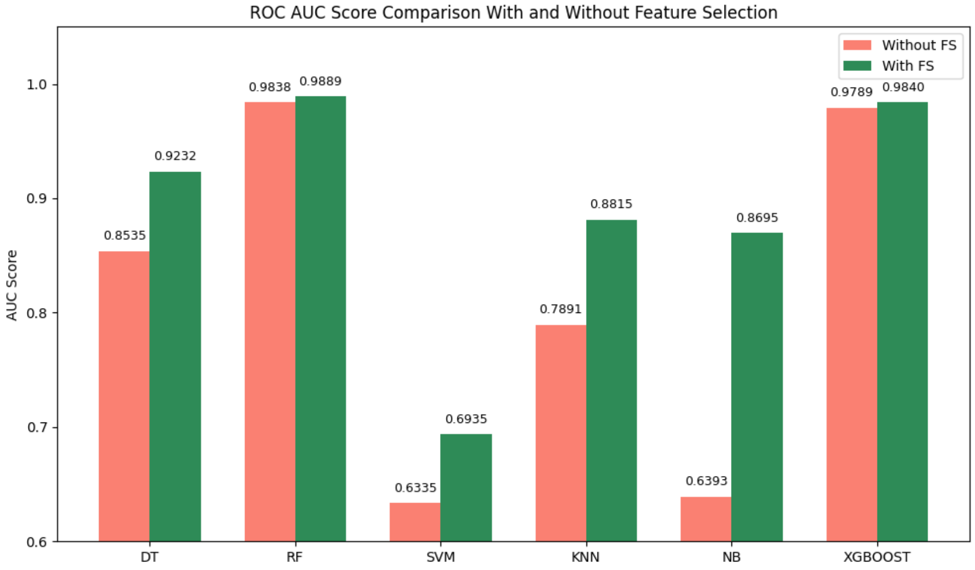

Fig. 2: Graphical illustrating the comparison of AUC with and without FS

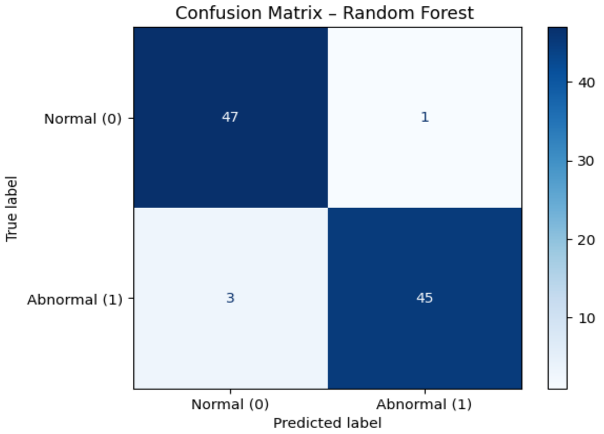

Fig. 3: Confusion matrix for the highest performing classifier for classification of pediatric kidney ultrasound images

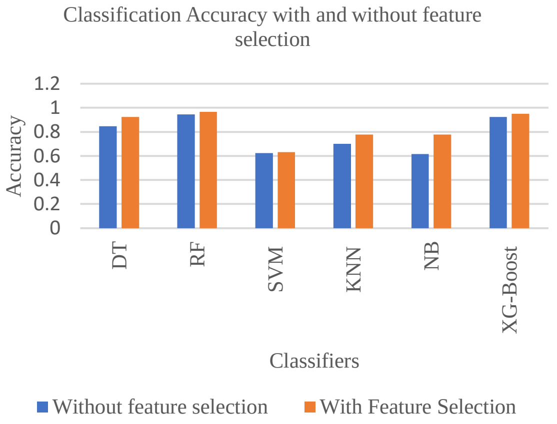

Fig. 4: Represent the classification accuracy with and without feature selection

Table 6: Performance metrics of the classifiers with and without FS

	Classifier	Accuracy	Precision	Recall	F-measure	Roc	Specificity
Without FS	DT	0.8462	0.8356	0.8714	0.8531	0.8535	0.8356
	RF	0.9441	0.9286	0.9286	0.9286	0.9838	0.9315
	SVM	0.6224	0.5816	0.8143	0.6786	0.6335	0.4384
	KNN	0.6993	0.7143	0.6429	0.6767	0.7891	0.7534
	NB	0.6154	0.6364	0.5000	0.5600	0.6393	0.7260
	XG-Boost	0.9231	0.9275	0.9143	0.9209	0.9789	0.9315
With FS (BinCOWmv)	DT	0.9231	0.9155	0.9286	0.9220	0.9232	0.9178
	RF	0.9650	0.9851	0.9429	0.9635	0.9889	0.9863
	SVM	0.6314	0.5730	0.7286	0.6415	0.6935	0.4795
	KNN	0.7762	0.8393	0.6714	0.7460	0.8815	0.8767
	NB	0.7762	0.7159	0.9000	0.7975	0.8695	0.6575
	XG-Boost	0.9510	0.9565	0.9429	0.9496	0.9840	0.9589

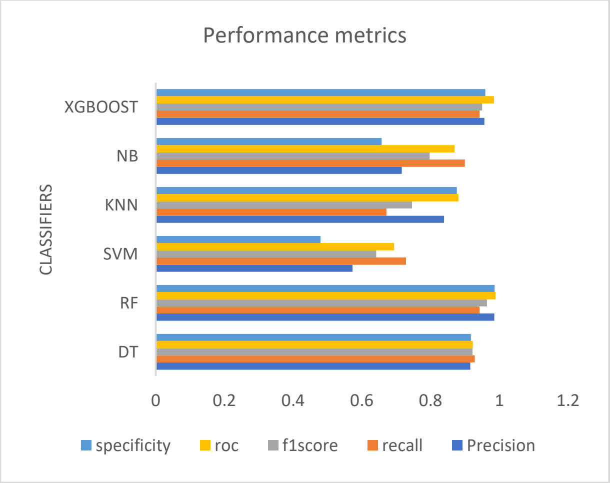

Fig. 5: Performance metrics for proposed method across different classifiers

Discussion

A comparative study evaluated the proposed approach against metaheuristic algorithms, including Coati optimization (COA), vector-weighted averaging (INFO), FireFly Algorithm (FFA), Harris Hawk optimization (HHO) and BinCoWvm. The Parameter settings are listed in Table 4, while Table 7 shows classification accuracies across six classifiers. The Results show that BinCoWmv outperforms all benchmark optimizers. The Decision Tree classifier accuracy increased from 84.62 to 92.31% with BinCoWmv, outperforming HHO and COA. Random Forest achieved 96.50% accuracy, surpassing HHO's 95.80%. BinCoWmv increases the BinCoWmv.

of the model by improving feature relevance and compactness. K-nearest neighbors showed significant improvements, whereas Naive Bayes improved owing to irrelevant feature removal. XG-Boost with BinCoWmv achieved higher accuracy than INFO and HHO. Table 8 shows BinCoWmv achieved the highest average fitness (0.94775) and lowest standard deviation (0.00404), indicating robustness. Its higher average feature count balances the compactness and representation. Although INFO showed faster convergence, it retained more features. The computational time of BinCoWmv was moderate, shorter than HHO, FFA, and COA. Statistical validation using the Friedman test showed a p-value of 0.0530. While HHO, INFO, and FFA achieved p values below 0.01, BinCoWmv higher p value indicated improved consistency. The 95% confidence interval ranged from 0.9472 to 0.9491 over 30 iterations. Table 9 shows that BinCoWmv with RF achieved 96.50% accuracy, outperforming PCA+ANN (77.89%), CSA+ANN, PCA+VGG16, and OGOA+ANN classifiers.

Table 7: Comparison of accuracies across different optimization algorithms

Classifiers	Without feature selection	With Coati features	With INFO features	With FFA features	with HHO features	with BinCoWmv features
DT	0.8462	0.8881	0.8392	0.7902	0.9091	0.9231
RF	0.9441	0.9301	0.9441	0.9091	0.958	0.965
SVM	0.6224	0.6014	0.6643	0.5664	0.5944	0.6014
KNN	0.6993	0.7413	0.5664	0.6993	0.6573	0.7762
NB	0.6154	0.6713	0.6783	0.6853	0.6783	0.7762
XG-Boost	0.9231	0.9091	0.9161	0.9091	0.9441	0.9510

Table 8: Value of mean, STD, Best fit, Worst fit, Avg Feature count, Avg Solution time, P-value, Confidence interval determined by BinCoWmv against original optimization algorithms

Optimization algo	Mean fitness	Std fitness	Best fit	Worst fit	Avg feature count	Avg solution time	p-value	Confidence interval
BinCoWmv	0.94775	0.00404	94.0659	92.1875	0.01657	123.75	0.053043	0.9472, 0.9491
Coati	0.90567	0.001338	88.89090	89.68688	0.03487	133.78	0.053044	0.9053, 0.9062
INFO	0.95670	0.000767	87.56778	87.97567	0.25087	112.52	0.004720	0.9573, 0.9570
FFA	0.86977	0.005977	86.63587	86.52454	0.56897	145.63	0.000228	0.8671, 0.8710
HHO	0.88460	0.006897	87.57878	89.57556	0.27076	139.08	0.004720	0.8822, 0.8872

Table 8: Comparison of proposed method with existing state-of-art

Ref.	Features	Method	Classification	Accuracy
(Priyanka and Kumar, 2020)	GLCM, 44 features	PCA	ANN	77.8%
(Nithya *et al.*, 2020)	GLCM, 22 features	CSA	ANN	93.45%
(Alkordy *et al.*, 2023)	VGG16 features	PCA	VGG16	95%
(Balamurugan and Arumugam, 2020)	GLCM, 22 features	OGOA	ANN	95.83%
Proposed	GLCM, GLRLM, GLSZM, GLDM, NGTDM, FIRST ORDER, 94 features	BinCoWmv optimization algorithm	RF	96.50%

Conclusion

Feature Selection (FS) can substantially enhance classification accuracy. This research presents a novel hybrid algorithm called Binary Coati and Weighted mean vector (BinCoWmv) optimization algorithm for classifying pediatric kidney ultrasound images. The methodology comprises five key stages: Initially, pediatric ultrasound images are acquired from an online repository. Next, these images are preprocessed to eliminate noise and artifacts, as well as to focus on the area of interest. The third step involves extracting radiomics features, with a focus on grey level characteristics of the ultrasound images. Subsequently, FS is performed, as not all extracted features are essential for classification due to the tissue-based nature of kidney structures. In this stage, metaheuristic optimization algorithms are utilized, specifically integrating coati optimization with a weighted mean vector (INFO), referred to as the BinCoWmv optimization algorithm. This approach enhances both exploration and exploitation abilities while preventing the algorithm from getting stuck in local optima. Initially operating in a continuous search space, the algorithm is subsequently converted into a binary search space tailored for the medical dataset. The subset of features that have been optimally chosen is subsequently classified using a range of classifiers, such as RF, DT, NB, KNN, SVM, and XG-Boost. The evaluation is based on confusion matrix parameters. The proposed method was evaluated against feature selection algorithms like Coati, INFO, FFA, and HHO. Results show this approach outperforms existing methods, delivering higher classification accuracy to support pediatric nephrologists in earlier detection of kidney abnormalities and improving patient outcomes. Future research directions include testing the proposed methodology with different larger dataset, assessing the feasibility of integrating the model into clinical workflows for real-time diagnostics assistance.

Acknowledgment

A heartfelt thanks to the university for providing resources to conduct the research.

Funding Information

The authors have not received any funding or financial support.

Author’s Contributions

Fizhan Kausar: Conceptualization, methodology, software, validation, resources, data curation, writing original draft preparation, formal analysis, investigation, writing review and edited.

Ramamurthy B.: Formal analysis, visualization, supervision.

Ethics

The manuscript presented here is new and contains unpublished content. All co-authors have reviewed and endorse the manuscript, as confirmed by the corresponding author. In addition, there are NO ethical concerns associated with this work.

References

Ahmad, R., & Mohanty, B. K. (2021). Chronic kidney disease stage identification using texture analysis of ultrasound images. *Biomedical Signal Processing and Control*, *69*, 102695. https://doi.org/10.1016/j.bspc.2021.102695

Ahmadianfar, I., Heidari, A. A., Noshadian, S., Chen, H., & Gandomi, A. H. (2022). INFO: An efficient optimization algorithm based on weighted mean of vectors. *Expert Systems with Applications*, *195*, 116516. https://doi.org/10.1016/j.eswa.2022.116516

Aljarah, I., Al-Zoubi, A. M., Faris, H., Hassonah, M. A., Mirjalili, S., & Saadeh, H. (2018). Simultaneous Feature Selection and Support Vector Machine Optimization Using the Grasshopper Optimization Algorithm. *Cognitive Computation*, *10*(3), 478–495. https://doi.org/10.1007/s12559-017-9542-9

Al-karawi, D., Al-Assam, H., Du, H., Sayasneh, A., Landolfo, C., Timmerman, D., Bourne, T., & Jassim, S. (2021). An Evaluation of the Effectiveness of Image-based Texture Features Extracted from Static B-mode Ultrasound Images in Distinguishing between Benign and Malignant Ovarian Masses. *Ultrasonic Imaging*, *43*(3), 124–138. https://doi.org/10.1177/0161734621998091

Alkordy, H., N., Aljobouri, H. K., & Kassim Wadi, Z. (2023). Feature Extraction and Selection of Kidney Ultrasound Images Using a Deep CNN and PCA. *Software Engineering Application in Systems Design*, *596*, 104–114. https://doi.org/10.1007/978-3-031-21435-6_10

Badawy, M., Almars, A. M., Balaha, H. M., Shehata, M., Qaraad, M., & Elhosseini, M. (2023). A two-stage renal disease classification based on transfer learning with hyperparameters optimization. *Frontiers in Medicine*, *10*, 1106717. https://doi.org/10.3389/fmed.2023.1106717

Bandara, M. S., Gurunayaka, B., Lakraj, G., Pallewatte, A., Siribaddana, S., & Wansapura, J. (2022). Ultrasound Based Radiomics Features of Chronic Kidney Disease. *Academic Radiology*, *29*(2), 229–235. https://doi.org/https://doi.org/10.1016/j.acra.2021.01.006

Barrera-García, J., Cisternas-Caneo, F., Crawford, B., Gómez Sánchez, M., & Soto, R. (2023). Feature Selection Problem and Metaheuristics: A Systematic Literature Review about Its Formulation, Evaluation and Applications. *Biomimetics*, *9*(1), 9. https://doi.org/10.3390/biomimetics9010009

Bhandari, M., Yogarajah, P., Kavitha, M. S., & Condell, J. (2023). Exploring the Capabilities of a Lightweight CNN Model in Accurately Identifying Renal Abnormalities: Cysts, Stones, and Tumors, Using LIME and SHAP. *Applied Sciences*, *13*(5), 3125. https://doi.org/10.3390/app13053125

Biradar, S., Akkasaligar, P. T., & Biradar, S. (2022). Feature Extraction and Classification of Digital Kidney Ultrasound Images: A Hybrid Approach. *Pattern Recognition and Image Analysis*, *32*(2), 363–372. https://doi.org/10.1134/s1054661822020043

Deepika, J., Selvaraju, P., Kumar Thota, M., Tiwari, M., Venu, D., Manjulaadevi, K., & Geetha Lakshmi, N. (2023). Efficient classification of kidney disease detection using Heterogeneous Modified Artificial Neural Network and Fruit Fly Optimization Algorithm. *Journal of Advanced Research in Applied Sciences and Engineering Technology*, *31*(3), 1–12. https://doi.org/10.37934/araset.31.3.112

Dehghani, M., Montazeri, Z., Trojovská, E., & Trojovský, P. (2023). Coati Optimization Algorithm: A new bio-inspired metaheuristic algorithm for solving optimization problems. *Knowledge-Based Systems*, *259*, 110011. https://doi.org/10.1016/j.knosys.2022.110011

Dyoub, A., & Letteri, I. (2023). Dataset Optimization for Chronic Disease Prediction with Bio-Inspired Feature Selection. *ArXiv.Org*, *1*, 12–15. https://doi.org/10.48550/arXiv.2401.05380

Dey, S., K., Mohammad Mohi Uddin, K., Hasan Babu, H. Md., Rahman, Md. M., Howlader, A., & Uddin, K. M. A. (2022). Chi2-MI: A hybrid feature selection based machine learning approach in diagnosis of chronic kidney disease. *Intelligent Systems with Applications*, *16*, 200144. https://doi.org/10.1016/j.iswa.2022.200144

Eid, H. F. (2018). Binary whale optimisation: An effective swarm algorithm for feature selection. *Inder Science*, *7*(1), 67–79. https://doi.org/10.1504/ijmheur.2018.091880

Emam, M. M., Houssein, E. H., Samee, N. A., Alohali, M. A., & Hosney, M. E. (2024). Breast cancer diagnosis using optimized deep convolutional neural network based on transfer learning technique and improved Coati optimization algorithm. *Expert Systems with Applications*, *255*, 124581. https://doi.org/10.1016/j.eswa.2024.124581

Francis, A., Harhay, M. N., Ong, A. C. M., Tummalapalli, S. L., Ortiz, A., Fogo, A. B., Fliser, D., Roy-Chaudhury, P., Fontana, M., Nangaku, M., Wanner, C., Malik, C., Hradsky, A., Adu, D., Bavanandan, S., Cusumano, A., Sola, L., Ulasi, I., Jha, V., … International Society of Nephrology. (2024). Chronic kidney disease and the global public health agenda: an international consensus. *Nature Reviews Nephrology*, *20*(7), 473–485. https://doi.org/10.1038/s41581-024-00820-6

Hao, S., Huang, C., Heidari, A. A., Chen, H., & Liang, G. (2024). An improved weighted mean of vectors optimizer for multi-threshold image segmentation: case study of breast cancer. *Cluster Computing*, *27*(10), 13945–14004. https://doi.org/10.1007/s10586-024-04491-7

Hashim, F. A., Houssein, E. H., Mostafa, R. R., Hussien, A. G., & Helmy, F. (2023). An efficient adaptive-mutated Coati optimization algorithm for feature selection and global optimization. *Alexandria Engineering Journal*, *85*, 29–48. https://doi.org/10.1016/j.aej.2023.11.004

Kausar, F., & Ramamurthy, B. (2023). Transforming Pediatric Healthcare with CKD using AI: A Systematic Mapping. *Proceedings of the IEEE International Conference*, 1–7. https://doi.org/10.1109/inc457730.2023.10263186

Kim, D.-H., & Ye, S.-Y. (2021). Classification of Chronic Kidney Disease in Sonography Using the GLCM and Artificial Neural Network. *Diagnostics*, *11*(5), 864. https://doi.org/10.3390/diagnostics11050864

Kou, J., Li, Z., You, Y., Wang, R., Chen, J., & Tang, Y. (2024). Automatic identification and classification of pediatric glomerulonephritis on ultrasound images based on deep learning and radiomics. *Journal of Big Data*, *11*(1), 165. https://doi.org/10.1186/s40537-024-01033-1

Lambert, J. R., & Perumal, E. (2022). Oppositional firefly optimization based optimal feature selection in chronic kidney disease classification using deep neural network. *Journal of Ambient Intelligence and Humanized Computing*, *13*(4), 1799–1810. https://doi.org/10.1007/s12652-021-03477-2

Mirjalili, S. (2016). Dragonfly algorithm: a new meta-heuristic optimization technique for solving single-objective, discrete, and multi-objective problems. *Neural Computing and Applications*, *27*(4), 1053–1073. https://doi.org/10.1007/s00521-015-1920-1

Mirjalili, S., & Lewis, A. (2013). S-shaped versus V-shaped transfer functions for binary Particle Swarm Optimization. *Swarm and Evolutionary Computation*, *9*, 1–14. https://doi.org/10.1016/j.swevo.2012.09.002

Nadimi-Shahraki, M. H., Asghari Varzaneh, Z., Zamani, H., & Mirjalili, S. (2022). Binary Starling Murmuration Optimizer Algorithm to Select Effective Features from Medical Data. *Applied Sciences*, *13*(1), 564. https://doi.org/10.3390/app13010564

Nithya, A., Appathurai, A., Venkatadri, N., Ramji, D. R., & Anna Palagan, C. (2020). Kidney disease detection and segmentation using artificial neural network and multi-kernel k-means clustering for ultrasound images. *Measurement*, *149*, 106952. https://doi.org/10.1016/j.measurement.2019.106952

Osama, S., Ali, A., & Shaban, H. (2023). A hybrid of Information gain and a Coati Optimization Algorithm for gene selection in microarray gene expression data classification. *Kafrelsheikh Journal of Information Sciences*, *4*(1), 1–16. https://doi.org/10.21608/kjis.2023.216661.1013

Patil, S., & Choudhary, S. (2024). Hybrid classification framework for chronic kidney disease prediction model. *The Imaging Science Journal*, *72*(3), 367–381. https://doi.org/10.1080/13682199.2023.2206272

Peng, L., Cai, Z., Heidari, A. A., Zhang, L., & Chen, H. (2023). Hierarchical Harris hawks optimizer for feature selection. *Journal of Advanced Research*, *53*, 261–278. https://doi.org/10.1016/j.jare.2023.01.014

Pradeepa, P., & Jeyakumar, M. K. (2023). Modelling of IDBN with LSNN based optimal feature selection for the prediction of CKD using real time data. *Multimedia Tools and Applications*, *82*(4), 6309–6344. https://doi.org/10.1007/s11042-022-13561-0

Priyanka, N., & Kumar, D. (2020). Feature Extraction and Selection of kidney Ultrasound Images Using GLCM and PCA. *Procedia Computer Science*, *167*, 1722–1731. https://doi.org/10.1016/j.procs.2020.03.382

Qtaish, A., Braik, M., Albashish, D., Alshammari, M. T., Alreshidi, A., & Alreshidi, E. J. (2025). Correction: Enhanced coati optimization algorithm using elite opposition-based learning and adaptive search mechanism for feature selection. *International Journal of Machine Learning and Cybernetics*, *16*(1), 395–395. https://doi.org/10.1007/s13042-024-02271-8

Raju, P., Malleswara Rao, V., & Prabhakara Rao, B. (2018). Grey Wolf Optimization-Based Artificial Neural Network for Classification of Kidney Images. *Journal of Circuits, Systems and Computers*, *27*(14), 1850231. https://doi.org/10.1142/s0218126618502316

Seyyedabbasi, A. (2023). Binary Sand Cat Swarm Optimization Algorithm for Wrapper Feature Selection on Biological Data. *Biomimetics*, *8*(3), 310. https://doi.org/10.3390/biomimetics8030310

Shankar, T. (2024). A Gallery of High-Resolution, Ultrasound, Color Doppler & 3D Images—Kidneys. *Ultrasound-Images*. https://www.ultrasound-images.com/?utm_source=copilot.com

Tian, S., Yu, Y., Shi, K., Jiang, Y., Song, H., Wang, Y., Yan, X., Zhong, Y., & Shao, G. (2024). Deep learning radiomics based on ultrasound images for the assisted diagnosis of chronic kidney disease. *Nephrology*, *29*(11), 748–757. https://doi.org/10.1111/nep.14376

Tsai, M.-C., Horng-Shing Lu, H. H.-S., Chang, Y.-C., Huang, Y.-C., & Fu, L.-S. (2022). Automatic Screening of Pediatric Renal Ultrasound Abnormalities: Deep Learning and Transfer Learning Approach. *JMIR Medical Informatics*, *10*(11), e40878. https://doi.org/10.2196/40878 van Griethuysen, J. J. M., Fedorov, A., Parmar, C., Hosny, A., Aucoin, N., Narayan, V., Beets-Tan, R. G. H., Fillion-Robin, J.-C., Pieper, S., & Aerts, H. J. W. L. (2017). Computational Radiomics System to Decode the Radiographic Phenotype. *Cancer Research, 77*(21), e104–e107. https://doi.org/10.1158/0008-5472.can-17-0339

Vasanthselvakumar, R., Balasubramanian, M., & Palanivel, S. (2017). Pattern Analysis of Kidney Diseases for Detection and Classification Using Ultrasound B-Mode Images. *International Journal of Pure and Applied Mathematics (IJPAM), 117*(15), 635–653.

Wang, X., Belkacem, A. N., Li, P., Zhang, Z., Liang, J., Du, D., & Chen, C. (2022). The Classification Method of EEG Motor Imagery Based on INFO-LSSVM. *Proceedings of the 2022 11th International Conference on Computing and Pattern Recognition*, 471–477. https://doi.org/10.1145/3581807.3581876

Wen, L., Yin, Q., & Guo, P. (2008). Ant Colony Optimization Algorithm for Feature Selection and Classification of Multispectral Remote Sensing Image. *Proceedings of the 2008 IEEE International Geoscience and Remote Sensing Symposium*, 915–918. https://doi.org/10.1109/igarss.2008.4779146

Wolpert, D. H., & Macready, W. G. (1997). *No free lunch theorems for optimization*. IEEE Transactions on Evolutionary Computation. https://doi.org/10.1109/4235.585893

Yildizdan, G., & Bas, E. (2024). A new binary coati optimization algorithm for binary optimization problems. *Neural Computing and Applications*, *36*(6), 2797–2834. https://doi.org/10.1007/s00521-023-09200-w